STABILIZED MIXED FINITE ELEMENT APPROXIMATION OF AXISYMMETRIC BRINKMAN FLOWS

VERÓNICA ANAYA*, DAVID MORA†, CARLOS REALES‡, AND RICARDO RUIZ-BAIER§

Dedicated to Rodolfo Rodríguez on his 60th birthday

Abstract. This paper is devoted to the numerical analysis of an augmented finite element approximation of the axisymmetric Brinkman equations. Stabilization of the variational formulation is achieved by adding suitable Galerkin least-squares terms, allowing us to transform the problem into a convenient formulation. The sought quantities (here velocity, vorticity, and pressure) are approximated by Raviart-Thomas elements of any order $k \geq 0$, piecewise continuous polynomials of degree $k+1$, and piecewise polynomials of degree k, respectively. The well-posedness of the resulting continuous and discrete variational problems is rigorously derived by virtue of the classical Babuška–Brezzi theory. We further establish a priori error estimates in the natural norms, and we provide a few numerical tests illustrating the behavior of the proposed augmented scheme and confirming our theoretical findings regarding optimal convergence of the approximate solutions.

Key words. Brinkman equations; Axisymmetric domains; Augmented mixed finite elements; Well-posedness analysis; Error estimates.

AMS subject classifications. 65N30; 65N12; 76D07; 65N15; 65J20.

1. Introduction. Cylindrical symmetry of both the data and the domain, very often allows transforming the original three-dimensional flow problem into a two-dimensional one, typically implying a substantial reduction in computational complexity. Apart from the advantages of considering an intrinsically axisymmetric problem in its natural configuration, such a reduction is particularly appealing in case of mixed approximations where additional unknowns are considered to accurately recover additional fields of physical interest. The attached difficulty usually resides in the analysis and derivation of proper schemes to discretize axisymmetric formulations, due to the presence of singularities associated to weighted functional spaces and their respective finite dimensional counterparts, which can eventually translate into numerical singularity near the rotation axis (considered as $(r = 0, z)$), since a factor of $1/r$ appears in all volume integrals.

The main purpose here is to propose and analyze an augmented mixed finite element method for the accurate discretization of the axisymmetric Brinkman problem in its vorticity-velocity-pressure formulation, which stands as prototype model for the study of Stokes and Darcy flow regimes and that can be employed to study semidiscretizations of transient Stokes problems. In addition, the vorticity (which is a scalar field in the axisymmetric case) is obtained directly from the formulation, without resorting to numerical postprocessing (prone to accuracy loss). Augmentation of the variational formulation with penalized residual-based terms, typically allows to recast the saddle point problem as a strongly elliptic system, and it also provides a way of bypassing the so-called kernel property, or to yield inf-sup stable continuous and discrete formulations (see for

*GIMNAP, Departamento de Matemática, Facultad de Ciencias, Universidad del Bío-Bío, Casilla 5-C, Concepción, Chile. Email: vanaya@ubiobio.cl. This author was partially supported by CONICYT-Chile through FONDECYT postdoctorado No.3120197, by project Inserción de Capital Humano Avanzado en la Academia No. 79112012, and DIUBB through project 120808 GI/EF.

†GIMNAP, Departamento de Matemática, Facultad de Ciencias, Universidad del Bío-Bío, Casilla 5-C, Concepción, Chile, and Centro de Investigación en Ingeniería Matemática (CI^{2}MA), Universidad de Concepción, Concepción, Chile. Email: dmora@ubiobio.cl. This author was partially supported by CONICYT-Chile through FONDECYT project 1140791, by DIUBB through project 120808 GI/EF, and Anillo ANANUM, ACT1118, CONICYT (Chile).

‡Corresponding author: Departamento de Matemáticas y Estadísticas, Universidad de Córdoba, Colombia. Email: creales@correo.unicordoba.edu.co.

§Institute of Earth Sciences, UNIL-Mouline Géopolis, University of Lausanne, CH-1015 Lausanne, Switzerland. Email: ricardo.ruizbaier@unil.ch. This author was supported by the Swiss National Science Foundation through the research grant PP00P2_144922.

instance, [21]). Our choice for the discretization of the governing equations is Raviart-Thomas elements of order k for the velocity field, piecewise continuous polynomials of degree $k+1$ for the vorticity, and piecewise discontinuous polynomials of degree k for the pressure field, for $k \geq 0$.

Related work and specifics of this contribution. There exist several references dealing with the mathematical and numerical analysis of axisymmetric problems. For instance, the strategy of reducing the dimension in finite element methods was used for the axisymmetric Laplace problem in the early work [32]. Later, several studies have been dedicated to different axisymmetric formulations of the Stokes equations employing finite differences [25, 31], and spectral, Mortar, Taylor-Hood, and stabilized finite elements (see [17, 8, 5, 11, 12, 13, 29, 30, 34]). Raviart-Thomas and Brezzi-Douglas-Marini mixed approximations for axisymmetric Darcy, and Stokes-Darcy flows were analyzed in [19, 20] using a generalization of the Stenberg criterion. Contributions focusing on numerical methods for axisymmetric formulations of flow and transport coupled problems can be found in e.g. [16, 26]. On the other hand, time-dependent and static Maxwell equations in axisymmetric singular domains were studied in [6, 7] by introducing a method based on a splitting of the space of solutions into a regular subspace and a singular one. In [28], a method was introduced to solve a time-harmonic Maxwell equation in axisymmetric domain using a Fourier decomposition. Such a technique was also employed in [32] for the axisymmetric Laplace equation. Up to our knowledge, the numerical analysis of finite element approximations of the generalized Stokes (or Brinkman) problem for the axisymmetric case has not been carried out yet. Nevertheless, in the Cartesian setting, there exist several methods including fully mixed, augmented, and stabilized formulations [9, 10, 23], whereas only a few recent contributions include formulations in terms of velocity, vorticity and pressure [3, 4, 36].

In this regard, we stress that the present study represents an extension to the vorticity-based Stokes problem analyzed in [2] in the sense that here we include the zeroth-order velocity component and introduce its axisymmetric formulation. On the other hand, the vorticity-based formulations for Brinkman equations analyzed in [3, 4, 36] are restricted to Cartesian two-dimensional domains, and therefore many practical applications remain out of reach. An axisymmetric flow model was derived from a three-dimensional scenario in [1], and the proposed numerical method was based on spectral finite elements. Here, we have chosen a different discretization since spectral approximations may exhibit some disadvantages in terms of accuracy in complex domains and in the presence of discontinuous coefficients, and their analysis typically requires higher regularity assumptions. These issues are no longer present in the scheme proposed herein.

Our analysis of existence and uniqueness of solution to the continuous axisymmetric problem is carried out by introducing an augmented formulation that arises from including penalized least-squares terms to the original variational formulation. We point out that this step is not necessary in the continuous case, but (as we will address in full detail) the presence of the term $1/r$ in the volume integrals requires some sort of stabilizing terms in the discrete formulation that would further allow us to relax constraints related to e.g. discrete inf-sup conditions. Thus, we opt for augmenting both continuous and discrete problems so that the same arguments can be applied for their solvability analysis. The tools employed to establish the convergence of our scheme consist in combining a Céa estimate with properties of the global Raviart-Thomas and Lagrange interpolation operators.

Outline. We have structured the contents of this paper as follows. The remainder of this Section introduces the classical Brinkman problem in Cartesian coordinates, along with its reduction to the axisymmetric case. We also present a mixed formulation for this problem, and summarize some preliminary results needed for its analysis. Section 2, is devoted to the statement of a least-squares-based augmented formulation to the axisymmetric generalized Stokes problem, and we perform the solvability analysis employing standard arguments from the Babuška-Brezzi theory. The mixed finite element formulation is presented in Section 3, where we also rigorously derive the stability analysis and optimal error estimates. We continue with a few illustrative numerical

examples collected in Section 4, which confirm the robustness and expected convergence properties of the proposed stabilized method, and we finally summarize the main aspects of this contribution in Section 5.

Cartesian Linear Brinkman equations. The linear Brinkman equations governing the motion of an incompressible fluid can be written as the following boundary value problem:

$$\sigma\breve{\boldsymbol{u}} - \nu\Delta\breve{\boldsymbol{u}} + \nabla\breve{p} = \breve{\boldsymbol{f}} \quad \text{in } \breve{\Omega}, \tag{1.1a}$$

$$\operatorname{div}\breve{\boldsymbol{u}} = 0 \quad \text{in } \breve{\Omega}, \tag{1.1b}$$

$$\breve{\boldsymbol{u}}\cdot\breve{\boldsymbol{n}} = 0 \quad \text{on } \partial\breve{\Omega}, \tag{1.1c}$$

$$\mathbf{curl}\,\breve{\boldsymbol{u}}\wedge\breve{\boldsymbol{n}} = 0 \quad \text{on } \partial\breve{\Omega}, \tag{1.1d}$$

where $\breve{\Omega}\subset\mathbb{R}^3$ is a given spatial domain. In this formulation, the sought quantities are the local volume-average velocity $\breve{\boldsymbol{u}}$ and the pressure field $\breve{p}$. The above system is also known as the generalized Stokes equations, and it allows in particular, to study spatial properties of the solutions to the time-dependent Stokes problem. In fact, the transient Stokes equations read

$$\partial_t\breve{\boldsymbol{u}} - \frac{1}{Re}\Delta\breve{\boldsymbol{u}} + \nabla\breve{p} = \breve{\boldsymbol{f}} \quad \text{in } \breve{\Omega}, \tag{1.2a}$$

$$\operatorname{div}\breve{\boldsymbol{u}} = 0 \quad \text{in } \breve{\Omega}, \tag{1.2b}$$

which, after applying a backward Euler time discretization of the acceleration term, yield to the following system

$$\frac{1}{\Delta t}\breve{\boldsymbol{u}}^{n+1} - \frac{1}{Re}\Delta\breve{\boldsymbol{u}}^{n+1} + \nabla\breve{p}^{n+1} = \breve{\boldsymbol{f}}^{n+1} + \frac{1}{\Delta t}\breve{\boldsymbol{u}}^{n} \quad \text{in } \breve{\Omega}, \tag{1.3a}$$

$$\operatorname{div}\breve{\boldsymbol{u}}^{n+1} = 0 \quad \text{in } \breve{\Omega}. \tag{1.3b}$$

That is, the solution of (1.2) requires to solve (1.3) at each time step.

When the data are axisymmetric, system (1.1a)-(1.1d) can be recast as two uncoupled problems in the so-called meridional domain Ω (see Figure 1.1): a problem involving only the unknown u_θ, and a problem with unknowns u_r, u_z and p. Here, we focus on the second case.

Preliminaries and axisymmetric formulation. In this section, we define appropriate weighted Sobolev spaces that will be used in the sequel and establish some of their properties; the corresponding proofs can be found in [11, 24, 32, 27]. More general results about weighted Sobolev spaces can be found in the last reference.

For an integer $\ell\geq 0$ and a real $1\leq q\leq\infty$, $L^q(\Omega)$ is the set of measurable functions φ such that $(\int_\Omega \varphi^q\,\mathrm{d}x\,)^{1/q}<\infty$ and $W^{\ell,q}(\Omega)$ denotes the usual Sobolev space of functions whose derivatives up to order ℓ are in $L^q(\Omega)$. Unless otherwise specified, we denote vector variables and spaces in bold.

In general, we will denote with $\breve{\ }$ a quantity associated to the three-dimensional domain $\breve{\Omega}$, whereas vector fields associated to the axisymmetric restriction will be denoted by $\boldsymbol{v}=(v_r,v_z)$. Let us also recall that the axisymmetric counterparts of the usual differential operators acting on vectors and scalars read

$$\operatorname{div}_{\mathrm{a}}\boldsymbol{v} := \partial_z v_z + \frac{1}{r}\partial_r(rv_r) = \partial_r v_r + r^{-1}v_r + \partial_z v_z, \qquad \operatorname{rot}\boldsymbol{v} := \partial_r v_z - \partial_z v_r,$$

$$\nabla\varphi := (\partial_r\varphi, \partial_z\varphi)^T, \qquad \mathbf{curl}_{\mathbf{a}}\,\varphi := (\partial_z\varphi, -r^{-1}\partial_r(r\varphi))^T.$$

After introducing the (scalar) vorticity field $\omega = \operatorname{rot}\boldsymbol{u}$, we notice that system (1.1a)-(1.1d) is equivalent to

$$\sigma\boldsymbol{u} + \nu\,\mathbf{curl}_{\mathbf{a}}\,\omega + \nabla p = \boldsymbol{f} \qquad \text{in } \Omega, \tag{1.4a}$$

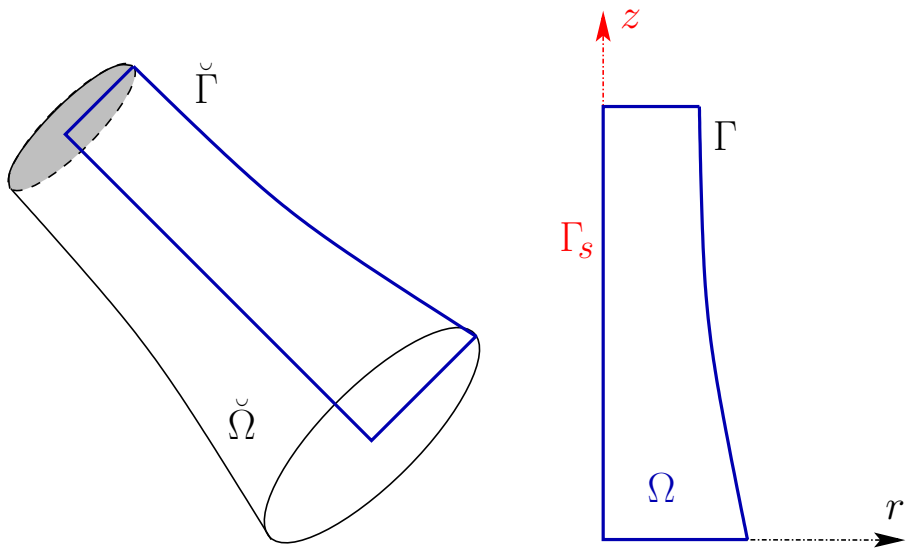

FIG. 1.1. *Sketch of a full three dimensional domain $\breve{\Omega}$ with boundary $\breve{\Gamma}$ and the axisymmetric meridional domain Ω with boundary Γ (left and right, respectively). Here Γ_s stands for the symmetry axis.*

$$\omega - \operatorname{rot} \boldsymbol{u} = 0 \qquad \text{in } \Omega, \tag{1.4b}$$

$$\operatorname{div}_{\mathrm{a}} \boldsymbol{u} = 0 \qquad \text{in } \Omega, \tag{1.4c}$$

$$\boldsymbol{u} \cdot \boldsymbol{n} = 0 \qquad \text{on } \Gamma, \tag{1.4d}$$

$$\omega = 0 \qquad \text{on } \Gamma. \tag{1.4e}$$

At times, we will need appropriate weighted Sobolev spaces which we introduce in what follows, along with some of their main properties; the corresponding proofs and further general results about weighted Sobolev spaces can be found in e.g. [11, 32, 27]. To alleviate the notation, we will denote the partial derivatives by ∂_r and ∂_z.

Let $\mathrm{L}^p_\alpha(\Omega)$ denote the weighted Lebesgue space of all measurable functions φ defined in Ω for which

$$\|\varphi\|_{\mathrm{L}^p_\alpha(\Omega)} := \int_\Omega |\varphi|^p \, r^\alpha \, \mathrm{d}r\mathrm{d}z \; < \infty.$$

The subspace $\mathrm{L}^2_{1,0}(\Omega)$ of $\mathrm{L}^2_1(\Omega)$ contains functions q with zero weighted integral:

$$\int_\Omega qr \, \mathrm{d}r\mathrm{d}z \; = 0.$$

The weighted Sobolev space $\mathrm{H}^k_r(\Omega)$ consists of all functions in $\mathrm{L}^2_1(\Omega)$ whose derivatives up to order k are also in $\mathrm{L}^2_1(\Omega)$. This space is provided with norms and semi-norms defined in the standard way; in particular,

$$|\varphi|^2_{\mathrm{H}^1_1(\Omega)} := \int_\Omega \left(|\partial_r \varphi|^2 + |\partial_z \varphi|^2 \right) r \, \mathrm{d}r\mathrm{d}z \, ,$$

and $\widetilde{\mathrm{H}}^1_1(\Omega) := \mathrm{H}^1_1(\Omega) \cap \mathrm{L}^2_{-1}(\Omega)$ endowed with the norm

$$\|\varphi\|_{\widetilde{\mathrm{H}}^1_1(\Omega)} := \left(|\varphi|^2_{\mathrm{H}^1_1(\Omega)} + \|\varphi\|^2_{\mathrm{L}^2_{-1}(\Omega)} \right)^{1/2},$$

is a Hilbert space. We will also require the following weighted spaces:

$$\mathrm{H}^1_{1,\diamond}(\Omega) := \left\{ \varphi \in \mathrm{H}^1_1(\Omega); \varphi = 0 \;\text{ on }\; \Gamma \right\},$$

$$
\begin{aligned}
\widetilde{\mathrm{H}}^1_{1,\diamond}(\Omega) &:= \left\{\varphi \in \widetilde{\mathrm{H}}^1_1(\Omega); \varphi = 0 \ \text{ on } \ \Gamma\right\},\\
\mathrm{H}(\mathrm{div_a},\Omega) &:= \left\{\boldsymbol{v} \in \mathrm{L}^2_1(\Omega)^2; \mathrm{div_a}\, \boldsymbol{v} \in \mathrm{L}^2_1(\Omega)\right\},\\
\mathrm{H}_0(\mathrm{div_a},\Omega) &:= \left\{\boldsymbol{v} \in \mathrm{L}^2_1(\Omega)^2; \mathrm{div_a}\, \boldsymbol{v} = 0 \ \text{ in } \ \Omega\right\},\\
\mathrm{H}_\diamond(\mathrm{div_a},\Omega) &:= \left\{\boldsymbol{v} \in \mathrm{H}(\mathrm{div_a},\Omega); \boldsymbol{v}\cdot\boldsymbol{n} = 0 \ \text{ on } \ \Gamma\right\},\\
\mathrm{H}(\mathbf{curl_a},\Omega) &:= \left\{\varphi \in \mathrm{L}^2_1(\Omega); \mathbf{curl_a}\, \varphi \in \mathrm{L}^2_1(\Omega)^2\right\},\\
\mathrm{H}(\mathrm{rot},\Omega) &:= \left\{\boldsymbol{v} \in \mathrm{L}^2_1(\Omega)^2; \mathrm{rot}\, \boldsymbol{v} \in \mathrm{L}^2_1(\Omega)\right\}.
\end{aligned}
$$

The spaces $\mathrm{H}(\mathrm{div_a},\Omega)$ and $\mathrm{H}(\mathbf{curl_a},\Omega)$ are endowed respectively by the norms:

$$
\begin{aligned}
\|\boldsymbol{v}\|_{\mathrm{H}(\mathrm{div_a},\Omega)} &:= \left(\|\boldsymbol{v}\|^2_{\mathrm{L}^2_1(\Omega)^2} + \|\,\mathrm{div_a}\,\boldsymbol{v}\|^2_{\mathrm{L}^2_1(\Omega)}\right)^{1/2},\\
\|\varphi\|_{\mathrm{H}(\mathbf{curl_a},\Omega)} &:= \left(\|\varphi\|^2_{\mathrm{L}^2_1(\Omega)} + \|\,\mathbf{curl_a}\,\varphi\|^2_{\mathrm{L}^2_1(\Omega)^2}\right)^{1/2}.
\end{aligned}
$$

In addition, notice that the norms $\|\cdot\|_{\mathrm{H}(\mathbf{curl_a},\Omega)}$ and $\|\cdot\|_{\widetilde{\mathrm{H}}^1_1(\Omega)}$ are equivalent, and for any $\varphi \in \widetilde{\mathrm{H}}^1_1(\Omega), \boldsymbol{v} \in \mathrm{H}(\mathrm{div_a},\Omega)$ they verify the following relations:

$$
\|\,\mathbf{curl_a}\,\varphi\|_{\mathrm{L}^2_1(\Omega)^2} \le \sqrt{2}\,\|\varphi\|_{\widetilde{\mathrm{H}}^1_1(\Omega)}, \tag{1.5}
$$

$$
\|\varphi\|_{\widetilde{\mathrm{H}}^1_1(\Omega)} \le \|\varphi\|_{\mathrm{H}(\mathbf{curl_a},\Omega)} \le \sqrt{3}\,\|\varphi\|_{\widetilde{\mathrm{H}}^1_1(\Omega)}, \tag{1.6}
$$

$$
\|\boldsymbol{v}\|^2_{\mathrm{H}(\mathrm{div_a},\Omega)} \le 2\left(\|v_r\|_{\widetilde{\mathrm{H}}^1_1(\Omega)} + \|v_z\|_{\mathrm{H}^1_1(\Omega)}\right)^2. \tag{1.7}
$$

We now collect some useful results to be employed in the sequel (see [1]).

LEMMA 1.1. *Let $H^{1/2}_1(\Gamma)$ be the trace space of functions in $\mathrm{H}^1_1(\Omega)$. The normal trace operator on Γ is defined by $\boldsymbol{v} \mapsto \boldsymbol{v}\cdot\boldsymbol{n}|_\Gamma$, and it is continuous from $\mathrm{H}(\mathrm{div_a},\Omega)$ into the dual space of $H^{1/2}_1(\Gamma)$.*

LEMMA 1.2. *For any $\boldsymbol{v} \in \mathrm{H}(\mathrm{div_a},\Omega)$ and $q \in \mathrm{H}^1_1(\Omega)$*

$$
\int_\Omega \mathrm{div_a}\,\boldsymbol{v} q r\,\mathrm{d}r\mathrm{d}z + \int_\Omega \boldsymbol{v}\cdot\nabla q r\,\mathrm{d}r\mathrm{d}z = \int_\Gamma \boldsymbol{v}\cdot\boldsymbol{n} q\,\mathrm{d}s.
$$

LEMMA 1.3. *For any $\boldsymbol{v} \in \mathrm{H}(rot,\Omega)$ and $\varphi \in \widetilde{\mathrm{H}}^1_1(\Omega)$*

$$
\int_\Omega \boldsymbol{v}\cdot\mathbf{curl_a}\,\varphi r\,\mathrm{d}r\mathrm{d}z - \int_\Omega \varphi\, rot\,\boldsymbol{v} r\,\mathrm{d}r\mathrm{d}z = \int_\Gamma \boldsymbol{v}\cdot\boldsymbol{t}\varphi\,\mathrm{d}s.
$$

Let us now test system (1.4a)-(1.4e) against functions $\boldsymbol{v} \in \mathrm{H}_\diamond(\mathrm{div_a},\Omega)$, $\varphi \in \widetilde{\mathrm{H}}^1_{1,\diamond}(\Omega)$ and $q \in \mathrm{L}^2_{1,0}(\Omega)$:

$$
\begin{aligned}
\sigma\int_\Omega \boldsymbol{u}\cdot\boldsymbol{v} r\,\mathrm{d}r\mathrm{d}z + \nu\int_\Omega \mathbf{curl_a}\,\omega\cdot\boldsymbol{v} r\,\mathrm{d}r\mathrm{d}z + \int_\Omega \nabla p\cdot\boldsymbol{v} r\,\mathrm{d}r\mathrm{d}z &= \int_\Omega \boldsymbol{f}\cdot\boldsymbol{v} r\,\mathrm{d}r\mathrm{d}z,\\
\int_\Omega \omega\varphi r\,\mathrm{d}r\mathrm{d}z - \int_\Omega \mathrm{rot}\,\boldsymbol{u}\varphi r\,\mathrm{d}r\mathrm{d}z &= 0,\\
\int_\Omega \mathrm{div_a}\,\boldsymbol{u} q r\,\mathrm{d}r\mathrm{d}z &= 0.
\end{aligned}
$$

Combining Lemmas 1.2 and 1.3 with a direct application of the boundary conditions yields

$$
\sigma\int_\Omega \boldsymbol{u}\cdot\boldsymbol{v} r\,\mathrm{d}r\mathrm{d}z + \nu\int_\Omega \mathbf{curl_a}\,\omega\cdot\boldsymbol{v} r\,\mathrm{d}r\mathrm{d}z - \int_\Omega \mathrm{div_a}\,\boldsymbol{v} p r\,\mathrm{d}r\mathrm{d}z = \int_\Omega \boldsymbol{f}\boldsymbol{v} r\,\mathrm{d}r\mathrm{d}z,
$$

$$\int_\Omega \omega\varphi r\,\mathrm{d}r\mathrm{d}z - \int_\Omega \boldsymbol{u}\cdot\mathbf{curl_a}\,\varphi r\,\mathrm{d}r\mathrm{d}z = 0,$$
$$\int_\Omega \mathrm{div_a}\,\boldsymbol{u}qr\,\mathrm{d}r\mathrm{d}z = 0.$$

This variational problem can be rewritten as follows: Find $(\boldsymbol{u},\omega,p)\in \mathrm{H}_\diamond(\mathrm{div_a},\Omega)\times\widetilde{\mathrm{H}}^1_{1,\diamond}(\Omega)\times \mathrm{L}^2_{1,0}(\Omega)$ such that

$$\begin{aligned} a(\boldsymbol{u},\boldsymbol{v})+b(\boldsymbol{v},\omega)+c(\boldsymbol{v},p) &= F(\boldsymbol{v}) && \forall \boldsymbol{v}\in \mathrm{H}_\diamond(\mathrm{div_a},\Omega),\\ b(\boldsymbol{u},\varphi)-d(\omega,\varphi) &= 0 && \forall \varphi\in \widetilde{\mathrm{H}}^1_{1,\diamond}(\Omega),\\ c(\boldsymbol{u},q) &= 0 && \forall q\in \mathrm{L}^2_{1,0}(\Omega), \end{aligned} \tag{1.8}$$

where the involved bilinear forms and linear functionals are defined as follows

$$a(\boldsymbol{u},\boldsymbol{v}) := \sigma\int_\Omega \boldsymbol{u}\cdot\boldsymbol{v}r\,\mathrm{d}r\mathrm{d}z\,,\qquad b(\boldsymbol{v},\omega) := \nu\int_\Omega \mathbf{curl_a}\,\omega\cdot\boldsymbol{v}r\,\mathrm{d}r\mathrm{d}z\,,$$
$$c(\boldsymbol{v},p) := -\int_\Omega \mathrm{div_a}\,\boldsymbol{v}pr\,\mathrm{d}r\mathrm{d}z\,,\quad d(\omega,\varphi) := \nu\int_\Omega \omega\varphi r\,\mathrm{d}r\mathrm{d}z\,,\quad F(\boldsymbol{v}) := \int_\Omega \boldsymbol{f}\cdot\boldsymbol{v}r\,\mathrm{d}r\mathrm{d}z\,.$$

2. A stabilized mixed formulation for the axisymmetric Brinkman problem. In this section, we will introduce and analyze a mixed variational formulation of the problem. We will propose an augmented dual-mixed variational formulation which will permit us to analyze the problem directly under the classical Babuška-Brezzi theory [15, 21].

2.1. Problem statement and preliminary results. Here, we propose an augmented dual-mixed variational formulation of system (1.4a)-(1.4e). Our strategy is to enrich the mixed variational formulation (1.8) with a residual arising from the equations (1.4a) and (1.4c).

More precisely, we add to the variational problem (1.8) the following Galerkin least-squares terms:

$$\kappa_1\int_\Omega (\sigma\boldsymbol{u}+\nu\,\mathbf{curl_a}\,\omega+\nabla p-\boldsymbol{f})\cdot\mathbf{curl_a}\,\varphi r\,\mathrm{d}r\mathrm{d}z = 0 \qquad \forall\varphi\in\widetilde{\mathrm{H}}^1_{1,\diamond}(\Omega), \tag{2.1}$$

$$\kappa_2\int_\Omega \mathrm{div_a}\,\boldsymbol{u}\,\mathrm{div_a}\,\boldsymbol{v}r\,\mathrm{d}r\mathrm{d}z = 0 \qquad \forall\boldsymbol{v}\in\mathrm{H}_\diamond(\mathrm{div_a},\Omega), \tag{2.2}$$

where κ_1 and κ_2 are positive parameters to be specified later. From Lemma 1.3, the fact that $\mathrm{rot}(\nabla p)=0$, and the boundary condition given in (1.4e), we may rewrite (2.1) equivalently as follows:

$$\kappa_1\sigma\int_\Omega \boldsymbol{u}\cdot\mathbf{curl_a}\,\varphi r\,\mathrm{d}r\mathrm{d}z + \kappa_1\nu\int_\Omega \mathbf{curl_a}\,\omega\cdot\mathbf{curl_a}\,\varphi r\,\mathrm{d}r\mathrm{d}z = \kappa_1\int_\Omega \boldsymbol{f}\cdot\mathbf{curl_a}\,\varphi r\,\mathrm{d}r\mathrm{d}z\,,$$

for all $\varphi\in\widetilde{\mathrm{H}}^1_{1,\diamond}(\Omega)$. In this way, and in addition to (1.8), we propose the following augmented variational formulation:

Find $((\boldsymbol{u},\omega),p)\in(\mathrm{H}_\diamond(\mathrm{div_a},\Omega)\times\widetilde{\mathrm{H}}^1_{1,\diamond}(\Omega))\times\mathrm{L}^2_{1,0}(\Omega)$ *such that*

$$\begin{aligned} A((\boldsymbol{u},\omega),(\boldsymbol{v},\varphi))+B((\boldsymbol{v},\varphi),p) &= G(\boldsymbol{v},\varphi) && \forall(\boldsymbol{v},\varphi)\in\mathrm{H}_\diamond(\mathrm{div_a},\Omega)\times\widetilde{\mathrm{H}}^1_{1,\diamond}(\Omega),\\ B((\boldsymbol{u},\omega),q) &= 0 && \forall q\in\mathrm{L}^2_{1,0}(\Omega), \end{aligned} \tag{2.3}$$

where the bilinear forms and the linear functional are defined by

$$A((\boldsymbol{u},\omega),(\boldsymbol{v},\varphi)) := \sigma\int_\Omega \boldsymbol{u}\cdot\boldsymbol{v}r\,\mathrm{d}r\mathrm{d}z + \nu\int_\Omega \mathbf{curl_a}\,\omega\cdot\boldsymbol{v}r\,\mathrm{d}r\mathrm{d}z - \nu\int_\Omega \mathbf{curl_a}\,\varphi\cdot\boldsymbol{u}r\,\mathrm{d}r\mathrm{d}z \tag{2.4}$$

$$
\begin{aligned}
&+ \nu \int_\Omega \omega\varphi r \,\mathrm{d}r\mathrm{d}z + \kappa_1\sigma \int_\Omega \boldsymbol{u}\cdot\mathbf{curl_a}\,\varphi r \,\mathrm{d}r\mathrm{d}z \\
&+ \kappa_1\nu \int_\Omega \mathbf{curl_a}\,\omega\cdot\mathbf{curl_a}\,\varphi r \,\mathrm{d}r\mathrm{d}z + \kappa_2 \int_\Omega \mathrm{div_a}\,\boldsymbol{u}\,\mathrm{div_a}\,\boldsymbol{v} r \,\mathrm{d}r\mathrm{d}z\,, \\
B((\boldsymbol{v},\varphi),q) &:= -\int_\Omega q\,\mathrm{div_a}\,\boldsymbol{v} r \,\mathrm{d}r\mathrm{d}z\,,
\end{aligned}
\tag{2.5}
$$

and

$$
G(\boldsymbol{v},\varphi) := \kappa_1 \int_\Omega \boldsymbol{f}\cdot\mathbf{curl_a}\,\varphi r \,\mathrm{d}r\mathrm{d}z + \int_\Omega \boldsymbol{f}\cdot\boldsymbol{v} r \,\mathrm{d}r\mathrm{d}z\,,
$$

for all $(\boldsymbol{u},\omega),(\boldsymbol{v},\varphi)\in \mathrm{H}_\diamond(\mathrm{div_a},\Omega)\times\widetilde{\mathrm{H}}^1_{1,\diamond}(\Omega)$, and $q\in \mathrm{L}^2_{1,0}(\Omega)$.

2.2. Unique solvability of the stabilized formulation. Next, we will prove that our stabilized variational formulation (2.3) satisfies the hypotheses of the Babuška-Brezzi theory, which yields the unique solvability and continuous dependence on the data of this variational formulation.

First, we observe that the bilinear forms A and B, and the linear functional G are bounded. More precisely, there exist $C_1, C_2, C_3 > 0$ such that

$$
\begin{aligned}
|A((\boldsymbol{u},\omega),(\boldsymbol{v},\varphi))| &\le C_1 \|(\boldsymbol{u},\omega)\|_{\mathrm{H}(\mathrm{div_a},\Omega)\times\widetilde{\mathrm{H}}^1_1(\Omega)} \|(\boldsymbol{v},\varphi)\|_{\mathrm{H}(\mathrm{div_a},\Omega)\times\widetilde{\mathrm{H}}^1_1(\Omega)}, \\
|B((\boldsymbol{v},\varphi),q)| &\le C_2 \|(\boldsymbol{v},\varphi)\|_{\mathrm{H}(\mathrm{div_a},\Omega)\times\widetilde{\mathrm{H}}^1_1(\Omega)} \|q\|_{\mathrm{L}^2_1(\Omega)}, \\
|G(\boldsymbol{v},\theta)| &\le C_3 \|(\boldsymbol{v},\varphi)\|_{\mathrm{H}(\mathrm{div_a},\Omega)\times\widetilde{\mathrm{H}}^1_1(\Omega)}.
\end{aligned}
$$

The following lemma shows that the bilinear form A is elliptic over the whole space $\mathrm{H}_\diamond(\mathrm{div_a},\Omega)\times\widetilde{\mathrm{H}}^1_{1,\diamond}(\Omega)$, provided that the stabilization parameters κ_1 and κ_2 are chosen adequately.

LEMMA 2.1. *Suppose that $\kappa_1\in(0,\frac{2\nu}{\sigma})$ and $\kappa_2>0$. Therefore, there exists $\alpha>0$, such that*

$$
A((\boldsymbol{v},\varphi),(\boldsymbol{v},\varphi)) \ge \alpha \|(\boldsymbol{v},\varphi)\|^2_{\mathrm{H}(\mathrm{div_a},\Omega)\times\widetilde{\mathrm{H}}^1_1(\Omega)} \qquad \forall (\boldsymbol{v},\varphi)\in \mathrm{H}_\diamond(\mathrm{div_a},\Omega)\times\widetilde{\mathrm{H}}^1_{1,\diamond}(\Omega).
$$

Proof. Given $(\boldsymbol{v},\varphi)\in \mathrm{H}_\diamond(\mathrm{div_a},\Omega)\times\widetilde{\mathrm{H}}^1_{1,\diamond}(\Omega)$, a combination of (2.4) with Cauchy-Schwarz inequality readily gives

$$
\begin{aligned}
A((\boldsymbol{v},\varphi),(\boldsymbol{v},\varphi)) =& \sigma\|\boldsymbol{v}\|^2_{\mathrm{L}^2_1(\Omega)^2} + \nu\|\varphi\|^2_{\mathrm{L}^2_1(\Omega)} + \kappa_1\sigma\int_\Omega \boldsymbol{v}\cdot\mathbf{curl_a}\,\varphi r\,\mathrm{d}r\mathrm{d}z \\
&+ \kappa_1\nu\|\mathbf{curl_a}\,\varphi\|^2_{\mathrm{L}^2_1(\Omega)^2} + \kappa_2\|\mathrm{div_a}\,\boldsymbol{v}\|^2_{\mathrm{L}^2_1(\Omega)}, \\
\ge& \sigma\|\boldsymbol{v}\|^2_{\mathrm{L}^2_1(\Omega)^2} + \nu\|\varphi\|^2_{\mathrm{L}^2_1(\Omega)} - \kappa_1\sigma\|\boldsymbol{v}\|_{\mathrm{L}^2_1(\Omega)^2}\|\mathbf{curl_a}\,\varphi\|_{\mathrm{L}^2_1(\Omega)^2} \\
&+ \kappa_1\nu\|\mathbf{curl_a}\,\varphi\|^2_{\mathrm{L}^2_1(\Omega)^2} + \kappa_2\|\mathrm{div_a}\,\boldsymbol{v}\|^2_{\mathrm{L}^2_1(\Omega)}, \\
\ge& \sigma\|\boldsymbol{v}\|^2_{\mathrm{L}^2_1(\Omega)^2} + \nu\|\varphi\|^2_{\mathrm{L}^2_1(\Omega)} - \frac{\sigma}{2}\|\boldsymbol{v}\|^2_{\mathrm{L}^2_1(\Omega)^2} - \frac{\kappa_1^2\sigma}{2}\|\mathbf{curl_a}\,\varphi\|^2_{\mathrm{L}^2_1(\Omega)^2} \\
&+ \kappa_1\nu\|\mathbf{curl_a}\,\varphi\|^2_{\mathrm{L}^2_1(\Omega)^2} + \kappa_2\|\mathrm{div_a}\,\boldsymbol{v}\|^2_{\mathrm{L}^2_1(\Omega)}, \\
=& \frac{\sigma}{2}\|\boldsymbol{v}\|^2_{\mathrm{L}^2_1(\Omega)^2} + \kappa_2\|\mathrm{div_a}\,\boldsymbol{v}\|^2_{\mathrm{L}^2_1(\Omega)} + \nu\|\varphi\|^2_{\mathrm{L}^2_1(\Omega)} \\
&+ \kappa_1\left(\nu - \frac{\kappa_1\sigma}{2}\right)\|\mathbf{curl_a}\,\varphi\|^2_{\mathrm{L}^2_1(\Omega)^2}, \\
\ge& \min\{\frac{\sigma}{2},\kappa_2\}\|\boldsymbol{v}\|^2_{\mathrm{H}(\mathrm{div_a},\Omega)} + \min\{\nu,\kappa_1\left(\nu-\frac{\kappa_1\sigma}{2}\right)\}\|\varphi\|^2_{\mathrm{H}(\mathbf{curl_a},\Omega)}, \\
\ge& \alpha\|(\boldsymbol{v},\varphi)\|^2_{\mathrm{H}(\mathrm{div_a},\Omega)\times\widetilde{\mathrm{H}}^1_1(\Omega)},
\end{aligned}
$$

where we have also employed (1.5). These steps complete the proof. ∎

The following result establishes the corresponding inf-sup condition for the bilinear form B (see (2.5)). Its proof is a direct consequence of the three-dimensional corresponding inf-sup condition (see [14, Lemma IX.1]) and estimate (1.7). For more details we refer to e.g. [1, Lemma 2.6].

LEMMA 2.2. *There exists $\beta > 0$, such that the following holds*

$$\sup_{\substack{(\boldsymbol{v},\varphi)\in \mathrm{H}_\diamond(\mathrm{div_a},\Omega)\times\widetilde{\mathrm{H}}^1_{1,\diamond}(\Omega)\\ (\boldsymbol{v},\varphi)\neq 0}} \frac{|B((\boldsymbol{v},\varphi),q)|}{\|(\boldsymbol{v},\varphi)\|_{\mathrm{H}(\mathrm{div_a},\Omega)\times\widetilde{\mathrm{H}}^1_1(\Omega)}} \geq \beta\|q\|_{\mathrm{L}^2_1(\Omega)} \quad \forall q \in \mathrm{L}^2_{1,0}(\Omega).$$

We are now in a position to state the main result of this section which yields the solvability of the continuous formulation (2.3).

THEOREM 2.3. *There exists a unique solution $((\boldsymbol{u},\omega),p) \in (\mathrm{H}_\diamond(\mathrm{div_a},\Omega)\times\widetilde{\mathrm{H}}^1_{1,\diamond}(\Omega))\times\mathrm{L}^2_{1,0}(\Omega)$ to problem (2.3) and there exists a positive constant $C > 0$ such that the following continuous dependence result holds:*

$$\|((\boldsymbol{u},\omega),p)\|_{(\mathrm{H}(\mathrm{div_a},\Omega)\times\widetilde{\mathrm{H}}^1_1(\Omega))\times\mathrm{L}^2_1(\Omega)} \leq C\|\boldsymbol{f}\|_{\mathrm{L}^2_1(\Omega)^2}.$$

Proof. By virtue of Lemmas 2.1 and 2.2, the proof follows from a straightforward application of [15, Theorem II.1.1]. ∎

3. Mixed finite element approximation. In this section, we construct a finite element scheme associated to (2.3), define explicit finite element subspaces yielding the unique solvability of the discrete scheme, derive the a priori error estimates, and provide the rate of convergence of the method.

3.1. Statement of the discrete scheme. Let $\{\mathcal{T}_h\}_{h>0}$ be a regular family of triangulations of Ω by triangles T with mesh size h. For $S \subset \bar{\Omega}$, we denote by $\mathbb{P}_k(S)$ and $\widetilde{\mathbb{P}}_k(S)$, $k \in \mathbb{N}\cup\{0\}$, the set of polynomials of degree $\leq k$, and the set of homogeneous polynomials of degree k on S, respectively. We begin by introducing some notation and basic definitions presented in [19]. First, we recall the definition of the two-dimensional Raviart-Thomas spaces, next we focus on the axisymmetric case. Let $\mathcal{E}_h$ be the set of all edges of the triangulation $\mathcal{T}_h$, and given $T \in \mathcal{T}_h$, let $\mathcal{E}(T)$ be the set of its edges, and we define the space

$$R_k(\partial T) := \{\phi \in \mathrm{L}^2(\partial T) : \phi_{|e} \in \mathbb{P}_k(e),\ e \in \mathcal{E}(T)\}.$$

For $\Omega \subset \mathbb{R}^2$, $T \in \mathcal{T}_h$, let us denote by $\mathrm{RT}_k(T)$ the Raviart-Thomas space, which is defined by

$$\mathrm{RT}_k(T) := \mathbb{P}_k(T)^2 + \begin{bmatrix} r \\ z \end{bmatrix} \widetilde{\mathbb{P}}_k(T),$$

where, for $\boldsymbol{v} \in \mathrm{RT}_k(T)$, $\boldsymbol{n}_T$ the unit outer normal on ∂T, the degrees of freedom are given by

$$\int_{\mathcal{E}(T)} \boldsymbol{v}\cdot\boldsymbol{n}_T\phi \qquad \forall \phi \in R_k(\partial T),$$

for $k \geq 0$, and

$$\int_T \boldsymbol{v}\cdot\boldsymbol{\phi} \qquad \forall \boldsymbol{\phi} \in \mathbb{P}_{k-1}(T)^2,$$

for $k \geq 1$. Regarding the axisymmetric case, we define $\mathcal{E}^{\mathrm{a}}(T)$ as the set of edges in the triangulation $\mathcal{T}_h$ contained in T, but which do not lie along the symmetry axis Γ_s. Additionally, we introduce the set

$$\mathcal{E}^{\mathrm{a}}(\mathcal{T}_h) := \cup_{T\in\mathcal{T}_h}\mathcal{E}^{\mathrm{a}}(T),$$

and define

$$\begin{aligned}\mathrm{RT}_k^{\mathrm{a}}(T) &:= \{\boldsymbol{v} \in \mathrm{RT}_k(T) : \boldsymbol{v}\cdot\boldsymbol{n}|_{\Gamma_s} = 0\}\\ &= \left\{ \begin{bmatrix} v_r \\ v_z \end{bmatrix} \in \mathrm{RT}_k(T) : v_r|_{\Gamma_s} = 0 \right\},\end{aligned}$$

where the degrees of freedom (for $k \geq 0$) are given by

$$\int_{\mathcal{E}(T)} \boldsymbol{v}\cdot\boldsymbol{n}_T \phi r \,\mathrm{d}r\mathrm{d}z \qquad \forall \phi \in R_k(\partial T),$$

and for $k \geq 1$, by

$$\int_T \boldsymbol{v}\cdot\boldsymbol{\phi} r \,\mathrm{d}r\mathrm{d}z \qquad \forall \boldsymbol{\phi} \in \mathbb{P}_{k-1}(T)^2.$$

Let us now make precise the choice of finite element subspaces, for any $k \geq 0$:

$$\mathrm{H}_h := \{\boldsymbol{v}_h \in \mathrm{H}_\diamond(\mathrm{div}_{\mathrm{a}},\Omega)\ \boldsymbol{v}_h|_T \in \mathrm{RT}_k^{\mathrm{a}}(T)\ \forall T \in \mathcal{T}_h\}, \tag{3.1}$$

$$\mathrm{Z}_h := \left\{\varphi_h \in \widetilde{\mathrm{H}}^1_{1,\diamond}(\Omega) :\ \varphi_h|_T \in \mathbb{P}_{k+1}(T)\ \forall T \in \mathcal{T}_h\right\}, \tag{3.2}$$

$$\mathrm{Q}_h := \left\{q_h \in \mathrm{L}^2_{1,0}(\Omega) :\ q_h|_T \in \mathbb{P}_k(T)\ \forall T \in \mathcal{T}_h\right\}. \tag{3.3}$$

Then, the Galerkin scheme associated with the continuous variational formulation (2.3) reads as follows:

Find $((\boldsymbol{u}_h,\omega_h),p_h) \in (\mathrm{H}_h \times \mathrm{Z}_h)\times \mathrm{Q}_h$ *such that*

$$\begin{aligned} A((\boldsymbol{u}_h,\omega_h),(\boldsymbol{v}_h,\varphi_h)) + B((\boldsymbol{v}_h,\varphi_h),p_h) &= G(\boldsymbol{v}_h,\varphi_h) \qquad \forall (\boldsymbol{v}_h,\varphi_h) \in \mathrm{H}_h\times\mathrm{Z}_h,\\ B((\boldsymbol{u}_h,\omega_h),q_h) &= 0 \qquad \forall q_h \in \mathrm{Q}_h.\end{aligned} \tag{3.4}$$

Remark 3.1. *Notice that the well-posedness of the continuous variational formulation* (1.8) *can be readily established using, for instance, the recent results from [22] related to a generalization of the Babuška-Brezzi theory (see also our Theorem 2.3). However, the discrete problem* (3.4) does not lie in such a framework *since the axisymmetric divergence of any* $\boldsymbol{v}_h \in \mathrm{H}_h$ *does not belong to* Q_h.

3.2. Solvability and stability of the stabilized discrete formulation. In view of Remark 3.1, we now devote ourselves to provide discrete counterparts of Lemmas 2.1 and 2.2, which will eventually conclude the solvability and stability of problem (3.4). With this aim, we first state the following result, which is a direct consequence of Lemma 2.1.

Lemma 3.1. *Assuming that* $\kappa_1 \in (0, \frac{2\nu}{\sigma})$ *and* $\kappa_2 > 0$, *then there exists* $\alpha > 0$, *such that*

$$A((\boldsymbol{v}_h,\varphi_h),(\boldsymbol{v}_h,\varphi_h)) \geq \alpha \|(\boldsymbol{v}_h,\varphi_h)\|^2_{\mathrm{H}(\mathrm{div}_{\mathrm{a}},\Omega)\times\widetilde{\mathrm{H}}^1_1(\Omega)} \qquad \forall (\boldsymbol{v}_h,\varphi_h) \in \mathrm{H}_h\times\mathrm{Z}_h.$$

We continue with the following discrete analogue to Lemma 2.2.

Lemma 3.2. *There exists* $\tilde{\beta} > 0$, *such that*

$$\sup_{\substack{(\boldsymbol{v}_h,\varphi_h)\in \mathrm{H}_h\times\mathrm{Z}_h\\ (\boldsymbol{v}_h,\varphi_h)\neq 0}} \frac{|B((\boldsymbol{v}_h,\varphi_h),q_h)|}{\|(\boldsymbol{v}_h,\varphi_h)\|_{\mathrm{H}(\mathrm{div}_{\mathrm{a}},\Omega)\times\widetilde{\mathrm{H}}^1_1(\Omega)}} \geq \tilde{\beta}\|q_h\|_{\mathrm{L}^2_1(\Omega)} \quad \forall q_h \in \mathrm{Q}_h.$$

Proof. Let $k \geq 0$ and $q_h \in \mathrm{Q}_h$. From Theorem 3.4 and Corollary 3.6 in [19], we know that there exist $\boldsymbol{v}_h \in \mathrm{H}_h$ and $\tilde{\beta} > 0$ such that,

$$\frac{\int_\Omega q_h \operatorname{div}_{\mathrm{a}} \boldsymbol{v}_h r \,\mathrm{d}r\mathrm{d}z}{\|\boldsymbol{v}_h\|_{\mathrm{H}(\operatorname{div}_{\mathrm{a}},\Omega)}} \geq \tilde{\beta}\|q_h\|_{\mathrm{L}^2_1(\Omega)}.$$

Therefore, from this inequality we have

$$\begin{aligned}\sup_{\substack{(\boldsymbol{v}_h,\varphi_h)\in \mathrm{H}_h\times \mathrm{Z}_h\\ (\boldsymbol{v}_h,\varphi_h)\neq 0}} \frac{|B((\boldsymbol{v}_h,\varphi_h),q_h)|}{\|(\boldsymbol{v}_h,\varphi_h)\|_{\mathrm{H}(\operatorname{div}_{\mathrm{a}},\Omega)\times\widetilde{\mathrm{H}}^1_1(\Omega)}} &\geq \frac{|B((\boldsymbol{v}_h,0),q_h)|}{\|(\boldsymbol{v}_h,0)\|_{\mathrm{H}(\operatorname{div}_{\mathrm{a}},\Omega)\times\widetilde{\mathrm{H}}^1_1(\Omega)}}\\ &= \frac{\int_\Omega q_h \operatorname{div}_{\mathrm{a}} \boldsymbol{v}_h r \,\mathrm{d}r\mathrm{d}z}{\|\boldsymbol{v}_h\|_{\mathrm{H}(\operatorname{div}_{\mathrm{a}},\Omega)}}\\ &\geq \tilde{\beta}\|q_h\|_{\mathrm{L}^2_1(\Omega)},\end{aligned}$$

which completes the proof. ∎

We are now in a position to state the main result of this section which yields the solvability of the discrete formulation (3.4).

THEOREM 3.3. *Let k be a non-negative integer and let H_h, Z_h and Q_h be given by (3.1), (3.2), and (3.3), respectively. Then, there exists a unique solution $((\boldsymbol{u}_h,\omega_h),p_h) \in (\mathrm{H}_h\times \mathrm{Z}_h)\times \mathrm{Q}_h$ to problem (3.4) and there exists a positive constant $C > 0$ such that the following continuous dependence result holds:*

$$\|((\boldsymbol{u}_h,\omega_h),p_h)\|_{(\mathrm{H}(\operatorname{div}_{\mathrm{a}},\Omega)\times\widetilde{\mathrm{H}}^1_1(\Omega))\times \mathrm{L}^2_1(\Omega)} \leq C\|\boldsymbol{f}\|_{\mathrm{L}^2_1(\Omega)^2}.$$

Moreover, there exists a constant $\widehat{C} > 0$ such that

$$\begin{aligned}&\|\boldsymbol{u}-\boldsymbol{u}_h\|_{\mathrm{H}(\operatorname{div}_{\mathrm{a}},\Omega)} + \|\omega-\omega_h\|_{\widetilde{\mathrm{H}}^1_1(\Omega)} + \|p-p_h\|_{\mathrm{L}^2_1(\Omega)}\\ &\qquad \leq \widehat{C}\left\{\inf_{\boldsymbol{v}_h\in \mathrm{H}_h}\|\boldsymbol{u}-\boldsymbol{v}_h\|_{\mathrm{H}(\operatorname{div}_{\mathrm{a}},\Omega)} + \inf_{\varphi_h\in \mathrm{Z}_h}\|\omega-\varphi_h\|_{\widetilde{\mathrm{H}}^1_1(\Omega)} + \inf_{q_h\in \mathrm{Q}_h}\|p-q_h\|_{\mathrm{L}^2_1(\Omega)}\right\},\end{aligned} \tag{3.5}$$

where $((\boldsymbol{u},\omega),p) \in (\mathrm{H}_\diamond(\operatorname{div}_{\mathrm{a}},\Omega)\times\widetilde{\mathrm{H}}^1_{1,\diamond}(\Omega))\times \mathrm{L}^2_{1,0}(\Omega)$ is the unique solution to problem (2.3).

Proof. By virtue of Lemmas 3.1 and 3.2, the proof follows from a straightforward application of [15, Theorem II.1.1]. ∎

3.3. Convergence analysis. According to the theorem above, there only remains to prove that $\boldsymbol{u}, \omega$ and p can be conveniently approximated by functions in $\mathrm{H}_h, \mathrm{Z}_h$ and Q_h respectively. With this purpose, we introduce the Raviart-Thomas global interpolation operator $\mathcal{R}_h : \mathrm{H}^1_1(\Omega) \to \mathrm{H}_h$ (see [19, Appendix]).

For this operator, we review some properties to be used in the sequel. The corresponding proofs can be found in [19, Corollary A.6]:

LEMMA 3.4. *For all $\boldsymbol{v} \in \mathrm{H}^{k+1}_1(\Omega)^2$, with $\operatorname{div}_{\mathrm{a}} \boldsymbol{v} \in \mathrm{H}^{k+1}_1(\Omega)$, and $\big(\sum_{T\in\mathcal{T}_h} |\operatorname{div}_{\mathrm{a}} \mathcal{R}_h\boldsymbol{v}|^2_{\mathrm{H}^{k+1}_1(T)}\big)^{1/2} < \tilde{c}$, there exists $C > 0$, independent of h, such that*

$$\|\boldsymbol{v}-\mathcal{R}_h\boldsymbol{v}\|_{\mathrm{H}(\operatorname{div}_{\mathrm{a}},\Omega)} \leq Ch^{k+1}.$$

Let $\mathcal{P}_h$ be the orthogonal projection from $\mathrm{L}^2_1(\Omega)$ onto the finite element subspace Q_h. We have that $\mathcal{P}_h$ satisfies the following error estimate (see [18]):

LEMMA 3.5. *There exists $C > 0$, independent of h, such that for all $q \in \mathrm{H}^{k+1}_1(\Omega)$:*

$$\|q-\mathcal{P}_h q\|_{\mathrm{L}^2_1(\Omega)} \leq Ch^{k+1}\|q\|_{\mathrm{H}^{k+1}_1(\Omega)}.$$

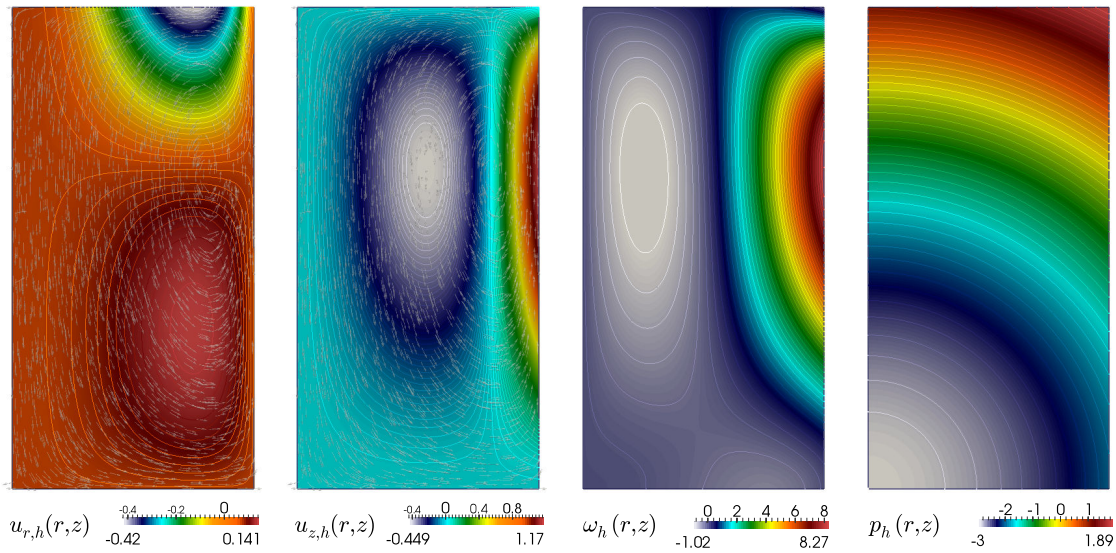

FIG. 3.1. *Approximate radial and longitudinal velocities, vorticity and pressure, obtained with lowest order Raviart-Thomas, piecewise linear, and piecewise constant elements, respectively. Errors with respect to the exact solutions in* (4.1) *are presented in Table 4.1.*

On the other hand, when the solution φ is sufficiently smooth, we are able to use the Lagrange interpolation operator $\Pi_h : \widetilde{\mathrm{H}}^1_1(\Omega) \cap \mathrm{H}^2_1(\Omega) \to \mathrm{Z}_h$. Moreover, there holds the following error estimate, whose proof can be found in [32, Lemma 6.3].

LEMMA 3.6. *There exists $C > 0$, independent of h, such that for all $\varphi \in \mathrm{H}^{k+2}_1(\Omega)$:*

$$\|\varphi - \Pi_h \varphi\|_{\widetilde{\mathrm{H}}^1_1(\Omega)} \leq C h^{k+1} \, \|\varphi\|_{\mathrm{H}^{k+2}_1(\Omega)} \, .$$

We are now in a position to establish the convergence properties of the discrete problem (3.4).

THEOREM 3.7. *Let k be a non-negative integer and let H_h, Z_h and Q_h be given by* (3.1), (3.2), *and* (3.3), *respectively. Let $((\boldsymbol{u},\omega),p) \in (\mathrm{H}_\diamond(\mathrm{div_a},\Omega) \times \widetilde{\mathrm{H}}^1_{1,\diamond}(\Omega)) \times \mathrm{L}^2_{1,0}(\Omega)$ and $((\boldsymbol{u}_h,\omega_h),p_h) \in (\mathrm{H}_h \times \mathrm{Z}_h) \times \mathrm{Q}_h$ be the unique solutions to the continuous and discrete problems* (2.3) *and* (3.4), *respectively. Assume that $\boldsymbol{u} \in \mathrm{H}^{k+1}_1(\Omega)$, $\mathrm{div_a}\, \boldsymbol{u} \in \mathrm{H}^{k+1}_1(\Omega)$, $\big(\sum_{T\in\mathcal{T}_h} |\, \mathrm{div_a}\, \mathcal{R}_h \boldsymbol{u}|^2_{\mathrm{H}^{k+1}_1(T)}\big)^{1/2} < \tilde{c}$, $\omega \in \mathrm{H}^{k+2}_1(\Omega)$, and $p \in \mathrm{H}^{k+1}_1(\Omega)$. Then, the following error estimate holds true*

$$\|\boldsymbol{u} - \boldsymbol{u}_h\|_{\mathrm{H}(\mathrm{div_a},\Omega)} + \|\omega - \omega_h\|_{\widetilde{\mathrm{H}}^1_1(\Omega)} + \|p - p_h\|_{\mathrm{L}^2_1(\Omega)} \leq C h^{k+1}.$$

Proof. The proof follows from (3.5) and error estimates from Lemmas 3.4, 3.5 and 3.6. ∎

Finally, we stress that our developed framework could be easily adapted to analyze other families of finite elements. For instance, considering BDM finite elements.

4. Numerical tests. In what follows, we present three numerical examples illustrating the performance of the FE method described in Section 3, and which confirm the theoretical error bounds.

4.1. Experimental convergence. We start by studying the accuracy of the proposed augmented formulation. This is carried out by computing errors in different norms, between the finite

d.o.f.	h	$\mathtt{e}(\omega_h)_{\widetilde{\mathrm{H}}^1_1(\Omega)}$	rate	$\mathtt{e}(\boldsymbol{u}_h)_{\mathrm{H}(\mathrm{div_a},\Omega)}$	rate	$\mathtt{e}(p_h)_{\mathrm{L}^2_1(\Omega)}$	rate
Augmented $\mathrm{RT}_0^a - \mathbb{P}_1 - \mathbb{P}_0$ finite elements							
19	1.414210	9.313142	–	2.196498	–	0.622498	–
61	0.707107	6.127531	0.643253	1.157689	0.887292	0.300841	1.049070
217	0.353553	3.230720	0.923452	0.606053	0.880587	0.157296	0.935521
817	0.176777	1.693433	0.931909	0.335337	0.879051	0.079495	0.984533
3169	0.088388	0.849415	0.995402	0.161066	0.947074	0.039855	0.996094
12481	0.044194	0.422061	1.009021	0.074841	1.105752	0.019941	0.998999
49537	0.022097	0.210592	1.003270	0.025636	1.054566	0.009972	0.999744
197377	0.011048	0.105225	1.000982	0.008879	1.052966	0.004986	0.999933
787969	0.005524	0.052590	1.000627	0.003592	1.130545	0.002493	0.999954
Augmented $\mathrm{RT}_1^a - \mathbb{P}_2 - \mathbb{P}_1$ finite elements							
47	1.414210	5.297575	–	5.771840	–	0.084158	–
152	0.707107	1.219981	2.118470	3.250071	0.954072	0.023349	1.849700
542	0.353553	0.387030	1.656351	0.738229	2.138333	0.005878	1.989971
2042	0.176777	0.102159	1.921632	0.122852	2.107151	0.001478	1.990832
7922	0.088388	0.025443	2.005452	0.018691	2.176473	0.000391	1.988041
31202	0.044194	0.006326	2.007954	0.002739	2.170384	9.950e-5	1.975634
123842	0.022097	0.001580	2.001371	0.000392	2.184897	2.310e-5	2.016722
493442	0.011048	0.000394	2.000989	6.098e-5	2.184340	6.177e-6	1.890525
1969922	0.005524	0.000179	2.000281	1.483e-5	2.098736	1.594e-6	1.975001

TABLE 4.1

Experimental convergence of the augmented $\mathbb{RT}_k^a - \mathbb{P}_{k+1} - \mathbb{P}_k$ FE approximation ($k = 0$, top rows, and $k = 1$ bottom rows) of the steady axisymmetric Brinkman flow with respect to exact solutions.

element approximation on successively refined non-uniform partitions $\mathcal{T}_h$ of Ω and the following exact solution to (1.4):

$$\begin{aligned} \boldsymbol{u}(r,z) &= \begin{pmatrix} r^3(r-1)z(3z-4) \\ -r^2(5r-4)z^2(z-2) \end{pmatrix}, \\ \omega(r,z) &= -z^2(z-2)r(15r-8) - r^3(r-1)(6z-4),\ p(r,z) = r^2+z^2-3, \end{aligned} \tag{4.1}$$

defined on the rectangular meridional domain $\Omega = (0,1)\times(0,2)$, and satisfying $\boldsymbol{u}\cdot\boldsymbol{n} = 0$ on $\Gamma\cup\Gamma_s$ and $\omega = 0$ on Γ_s. In this case, we impose a non-homogeneous Dirichlet condition for the vorticity on Γ, and the model and stabilization parameters are set as $\sigma = 0.1$, $\nu = 0.01$, $\kappa_1 = 0.5\nu/\sigma$, $\kappa_2 = 0.001$. The approximate solutions computed with the augmented formulation on a mesh with 263680 triangular elements are presented in Figure 3.1. We also compute rates of convergence from one refinement level (associated to a partition of size h) to the next one (with a mesh of size $\hat{h} < h$) as

$$\mathtt{rate}_h = \frac{\log(\mathtt{error}_h/\mathtt{error}_{\hat{h}})}{\log(h/\hat{h})}.$$

These values are displayed in Table 4.1, where we observe a convergence of order h^{k+1} for all fields in the relevant norms.

4.2. Axisymmetric Brinkman flow on a settling tank. In our next example, we simulate a common scenario in wastewater treatment processes, that is a settling tank, where the accurate rendering of flow is of interest. The geometry depicted in Figure 4.1 (see also [2, 16]) represents a half cross-section of a cylindrical vessel with the following types of boundaries: inlet Γ_{in}, outlet Γ_{out}, symmetry axis Γ_s, overflow Γ_c, and walls (the remainder of $\partial\Omega$).

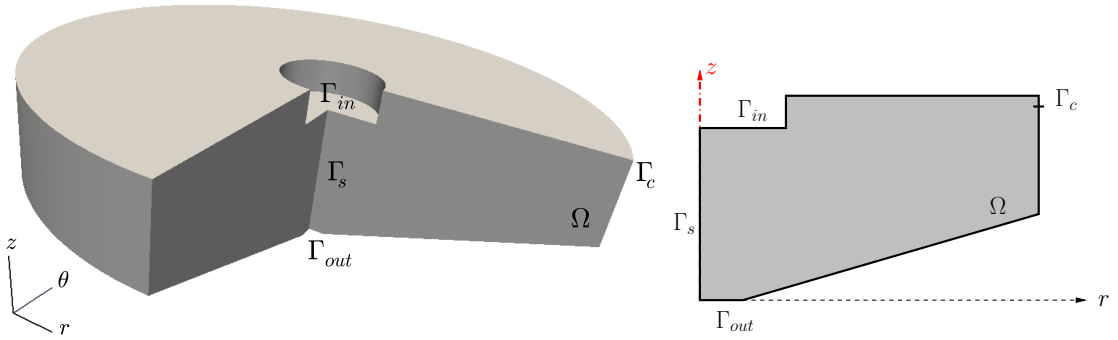

FIG. 4.1. *Sketch of a half cross section of a settling tank of maximum radius 8m, total height of 5m, inlet disk of 1.5m of radius, overflow annulus of 0.5m of edge, and outlet disk with a radius of 0.5m.*

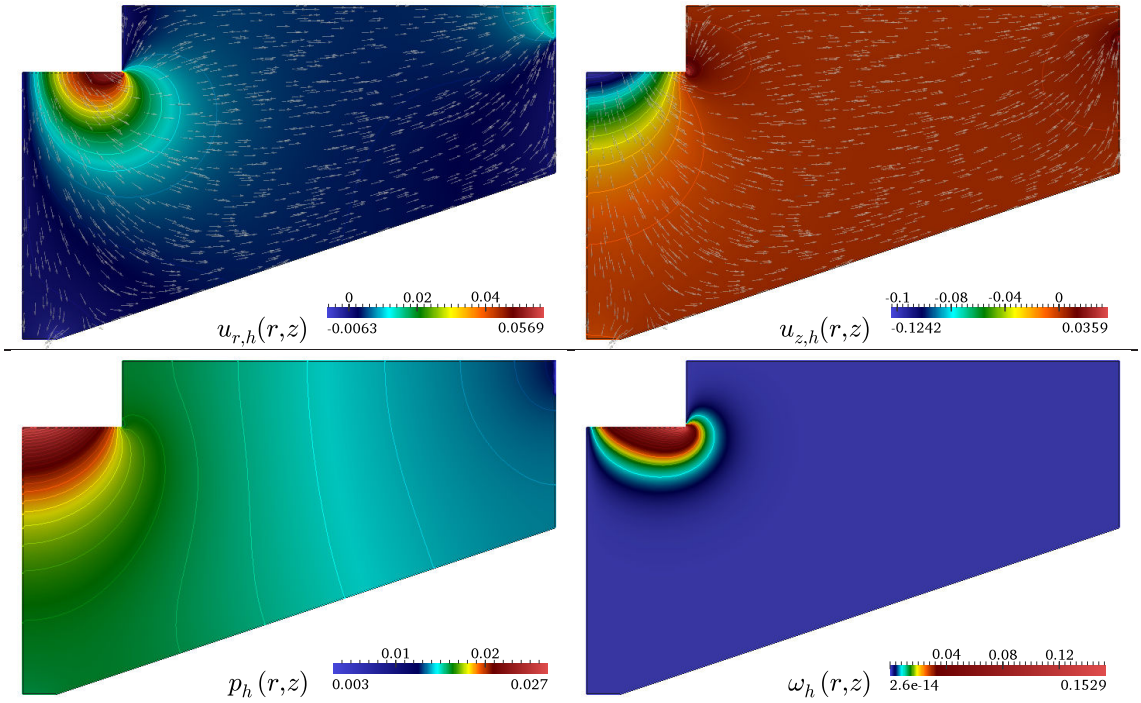

FIG. 4.2. *Approximate solutions of the Brinkman axisymmetric problem on a settling tank. The used mesh consists of 107882 elements.*

Boundary conditions assume the following configuration. On walls and symmetry axis we allow a slip velocity, that is $\boldsymbol{u} \cdot \boldsymbol{n} = 0$; normal velocities are imposed on the inlet, outlet and overflow as $q_{in} = \frac{1}{8}(\frac{4r^2}{9} - 1)$, $q_{out} = 0.01125$, $q_c = 0.00125$, respectively. Zero vorticity is imposed on the walls, symmetry axis, outlet and overflow, whereas on the inlet we set $w_{in} = \frac{r}{9}$. The external force is assumed to be zero.

An unstructured mesh of 107882 triangles and 54420 nodes was constructed, and we employed the following model and stabilization parameters: $\sigma = 0.1$, $\nu = 0.01$, $\kappa_1 = \nu/\sigma$, $\kappa_2 = 0.01$. Approximate radial and vertical components of the velocity, pressure and vorticity are displayed in Figure 4.2.

4.3. Blood flow through an axisymmetric stenosed artery. Next, we present the simulation of a simplified model of arterial blood flow in the presence of a symmetric stenotic region

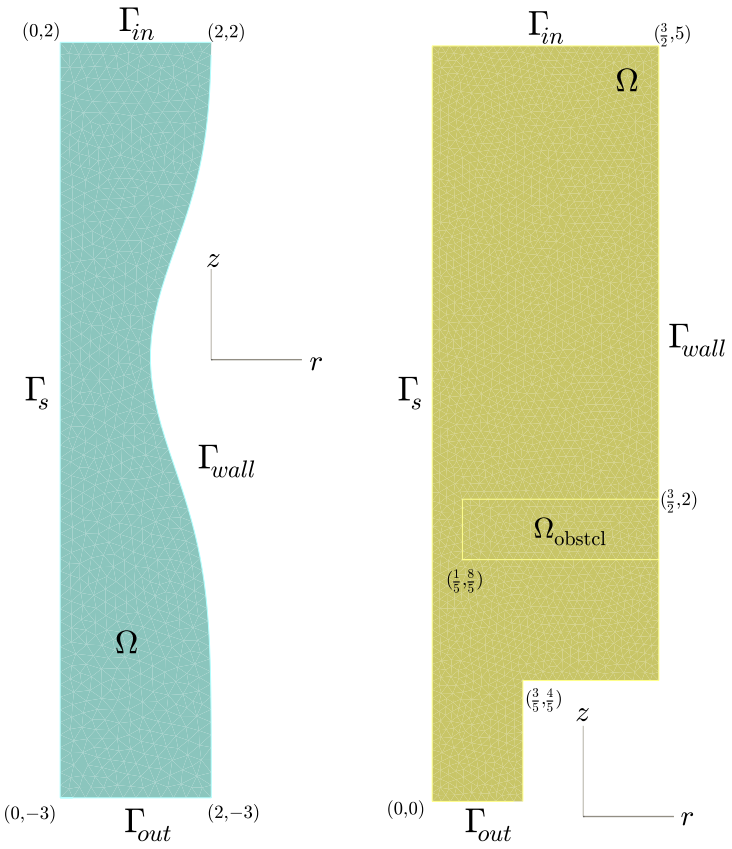

FIG. 4.3. *Sketch of a half cross section of an idealized artery with symmetric stenosis (left) and a cylindrical filter with sudden contraction (right).*

on the vessel wall (see e.g. [33, 35]). We are only interested in the laminar regime, so (1.1) (with a simple Newtonian model for the blood) will suffice to describe the main components of the flow. The computational domain consists on a half cross-section of a vessel segment of length 5cm and maximum radius 1cm (see a sketch in Figure 4.3, left). The boundaries are the inlet Γ_{in} ($z = 2$, $r \in [0,1]$) outlet Γ_{out} ($z = -3$, $r \in [0,1]$), symmetry axis Γ_s ($z \in [-3,2]$, $r = 0$), and arterial wall ($z \in [-3,2]$, $r = 1 + \delta \exp(-sz^2)(z+3)(z+2)/6$), with $\delta = 0.4$ and $s = 0.8$. Boundary data are set in the following manner: on Γ_{in} we impose a Poiseuille flow of maximum normal velocity with norm Re$= 1/\nu$, and a consistent vorticity $w = 2r/\nu$. On symmetry axis and arterial wall we set zero normal velocity and vorticity, whereas on the outlet we use $\boldsymbol{u} \cdot \boldsymbol{t} = 0$ and $p = 0$. The conditions on Γ_{out} were not covered in our analysis, but we stress that they can be also treated following e.g. [2, 3]. The flow regime is characterized by the parameters $\nu = 0.01$, and we set $\sigma = 0.01$, $\kappa_1 = \nu/\sigma$, $\kappa_2 = 0.1$. An unstructured mesh of 43712 elements and 21857 nodes was built to discretize the axisymmetric domain Ω. Figure 4.4 displays approximate solutions using Raviart-Thomas elements for velocity, piecewise linear and continuous elements for vorticity and piecewise constant elements for pressure. For visualization purposes, we also depict a rotational extrusion of 290 degrees of these solutions in Figure 4.5.

4.4. Flow in a contracting cylinder with porous obstacle. We close this section with a simulation relevant in the modeling of oil filters. We consider a cylindrical domain with a annular porous obstacle, whose half cross-section is depicted in the right panel of Figure 4.3, and assume that the permeability inside the obstacle Ω_{obstcl} is much lower than that of the rest of the domain.

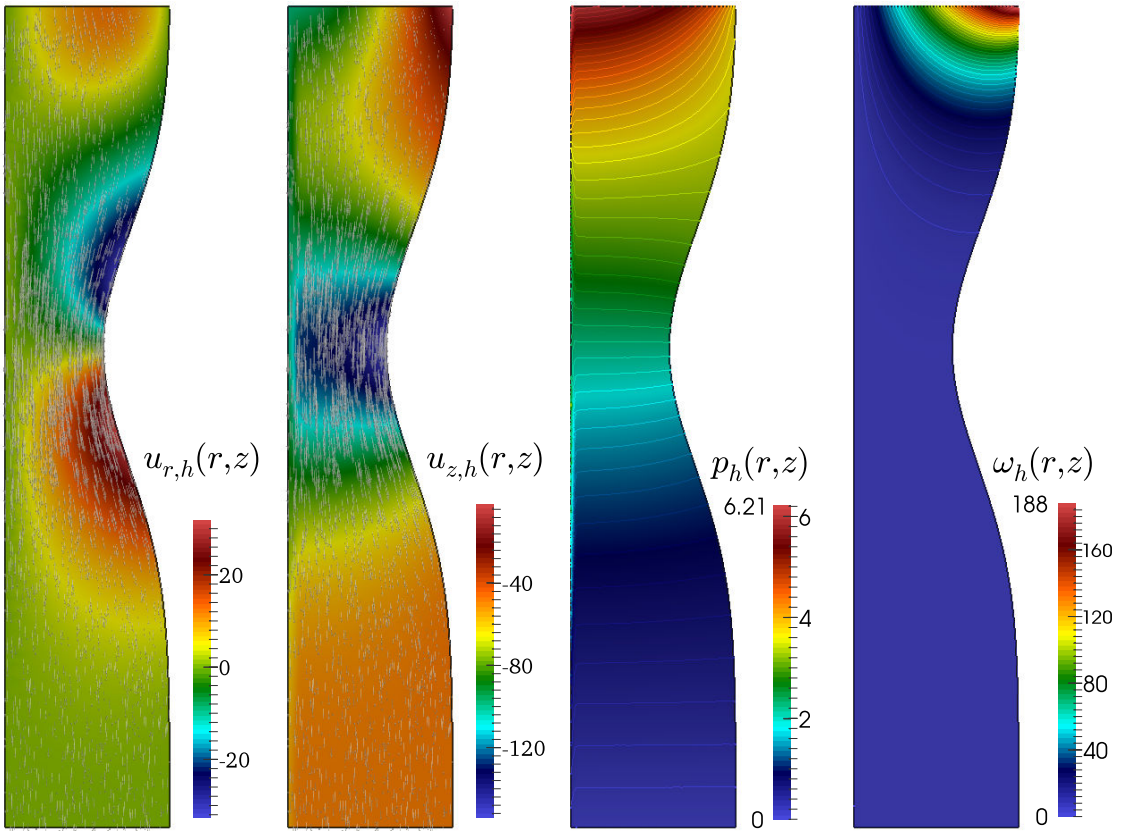

FIG. 4.4. *Augmented mixed finite element approximation of the Brinkman axisymmetric problem on a stenosed artery. Solutions on the half cross-section discretized with 43712 triangular elements.*

This assumption is accounted for by setting

$$\sigma = \sigma(r,\theta) = \begin{cases} \sigma_0 = 100 & \text{in } \Omega_{\text{obstcl}}, \\ \sigma_1 = 0.001 & \text{otherwise.} \end{cases}$$

As in the previous test case, we here impose the Poiseuille normal velocity inflow $\boldsymbol{u}\cdot\boldsymbol{n} = 2/75r(r-3/2)$ and the compatible vorticity $\omega = 2/75(r-3/2)$ on Γ_{in}, on Γ_s and Γ_{wall} we set zero normal velocity and vorticity, and on the outlet we do not constraint flow nor pressure. Other model parameters are chosen as $\nu = 0.01$, $\kappa_1 = 3/2\nu\sigma_0/\sigma_1^2$, $\kappa_2 = 0.1$, and $\boldsymbol{f} = \boldsymbol{0}$. The axisymmetric domain was discretized with an unstructured mesh of 122303 triangular elements and 61021 vertices.

The approximate solutions obtained with the proposed augmented finite element method are displayed in Figure 5.1. As expected (see a similar study for the Cartesian case in [3]), we can observe velocity patterns avoiding the annular porous obstacle and concentrating on the symmetry axis, and pressure profiles with high gradients near the obstacle boundary.

5. Conclusions. In this work, we have presented a new stabilized mixed finite element method for the discretization of the a vorticity-velocity-pressure formulation of the Brinkman problem in axisymmetric coordinates. A rigorous solvability analysis of both continuous and discrete problems was carried out using tools from the Babuška-Brezzi theory, and we derived optimal convergence rates in the natural norms for the particular case of Raviart-Thomas approximations of order k of velocities, and piecewise polynomials of degrees $k+1$ and k approximating the scalar vorticity and pressure, respectively. We provided a few numerical tests confirming our theoretical

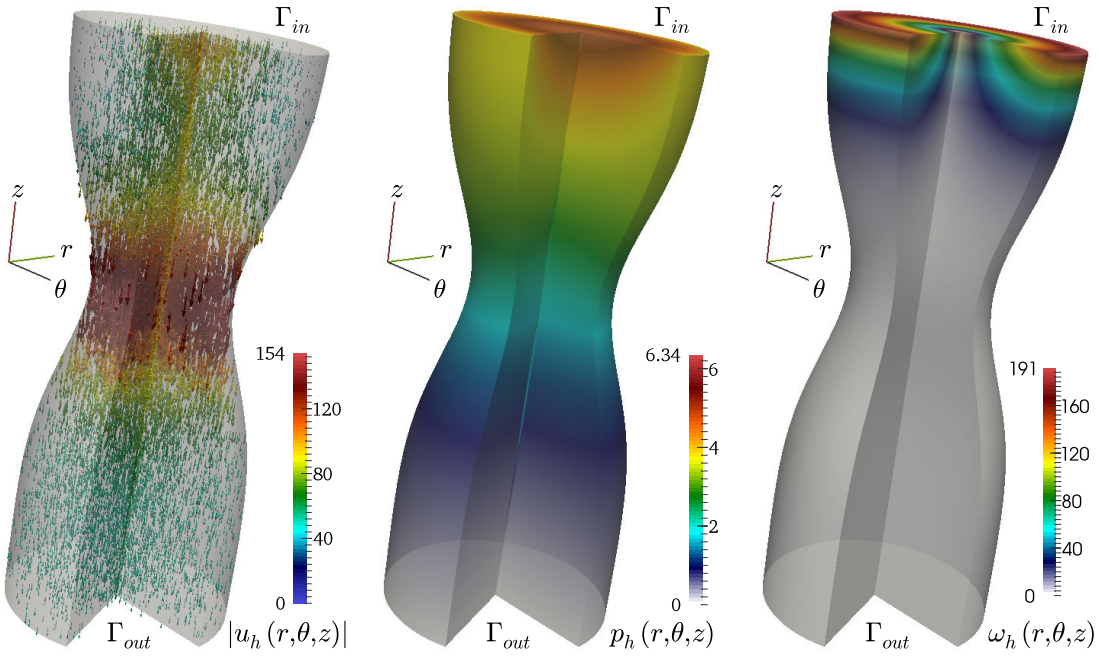

FIG. 4.5. *Augmented mixed finite element approximation of the Brinkman axisymmetric problem on a stenosed artery. Rotational extrusion to the full three-dimensional domain.*

findings regarding optimal convergence of the approximate solutions and showing that our framework can be successfully applied in a wide range of interesting applications as wastewater treatment processes, the simulation of arterial blood flow, and the modeling of oil filters. Possible extensions of this work include the study of vorticity-based formulations of axisymmetric time-dependent Navier-Stokes equations, the incorporation of a larger class of boundary conditions, and the use of the developed theory in the coupling of flow equations and nonlinear transport problems.

REFERENCES

[1] N. ABDELLATIF, N. CHORFI, AND S. TRABELSI, *Spectral discretization of the axisymmetric vorticity, velocity and pressure formulation of the Stokes problem*. J. Sci. Comput., **47** (2011) 419–440.

[2] V. ANAYA, D. MORA, AND R. RUIZ-BAIER, *An augmented mixed finite element method for the vorticity-velocity-pressure formulation of the Stokes equations*. Comput. Methods Appl. Mech. Engrg., **267** (2013) 261–274.

[3] V. ANAYA, D. MORA, G.N. GATICA, AND R. RUIZ-BAIER, *An augmented velocity-vorticity-pressure formulation for the Brinkman problem*. CI^{2}MA preprint 2014-11, available from `ci2ma.udec.cl/publicaciones/prepublicaciones`.

[4] V. ANAYA, D. MORA, R. OYARZÚA, AND R. RUIZ-BAIER, *Mixed velocity-vorticity-pressure formulation for the generalized Stokes problem*. In preparation.

[5] S.M. AOUADI, C. BERNARDI, AND J. SATOURI, *Mortar spectral element discretization of the Stokes problem in axisymmetric domains*. Numer. Methods Part. Diff. Eqns., **30** (2014) 44–73.

[6] F. ASSOUS, P. CIARLET, AND S. LABRUNIE, *Theoretical tools to solve the axisymmetric Maxwell equations*. Math. Methods Appl. Sci., **25** (2002) 49–78.

[7] F. ASSOUS, P. CIARLET, S. LABRUNIE, AND J. SEGRÉ, *Numerical solution to the time-dependent Maxwell equations in axisymmetric singular domains: the singular complement method*. J. Comput. Phys., **191** (2003) 147–176.

[8] M. AZAIEZ, *A spectral element projection scheme for incompressible flow with application to the unsteady axisymmetric Stokes problem*. J. Sci. Comput., **17** (2002) 573–584.

[9] G.R. BARRENECHEA, AND F. VALENTIN, *An unusual stabilized finite element method for a generalized Stokes problem*. Numer. Math., **92**(4) (2002) 653–677.

[10] T. BARRIOS, R. BUSTINZA, G. GARCÍA, AND E. HERNÁNDEZ, *On stabilized mixed methods for generalized Stokes problem based on the velocity-pseudostress formulation: a priori error estimates*. Comput. Methods Appl.

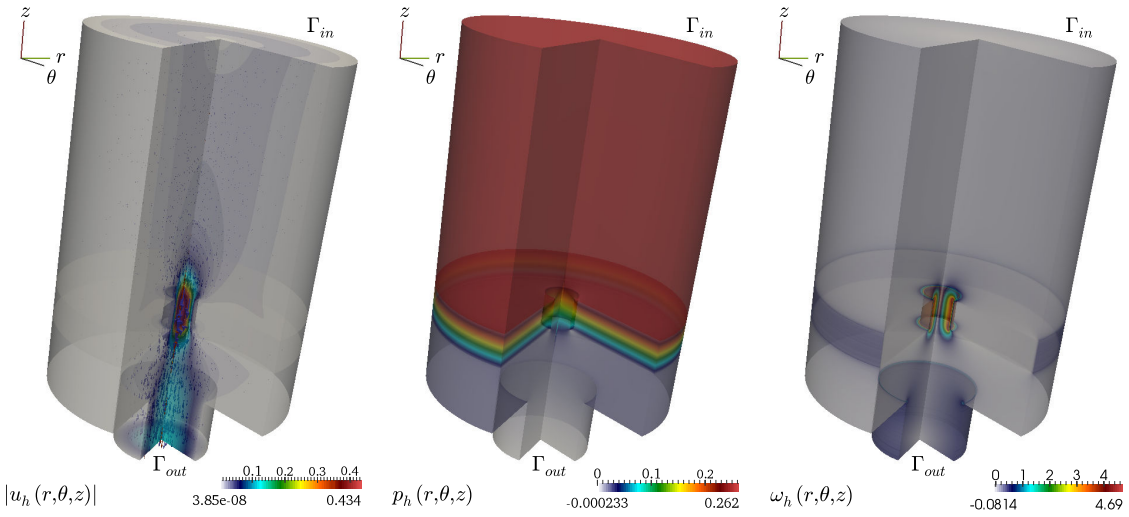

FIG. 5.1. *Augmented mixed finite element approximation of the Brinkman axisymmetric problem on an idealized oil filter. Rotational extrusion of velocity, pressure and vorticity (left, center, and right, respectively) to the full three-dimensional domain.*

Mech. Engrg., **237/240** (2012) 78–87.

[11] Z. Belhachmi, C. Bernardi, and S. Deparis, *Weighted Clément operator and application to the finite element discretization of the axisymmetric Stokes problem*. Numer. Math., **105** (2002) 217–247.

[12] Z. Belhachmi, C. Bernardi, S. Deparis, and F. Hecht, *An efficient discretization of the Navier-Stokes equations in an axisymmetric domain. Part 1: The discrete problem and its numerical analysis*. J. Sci. Comput., **27** (2006) 97–110.

[13] C. Bernardi, and N. Chorfi, *Spectral discretization of the vorticity, velocity, and pressure formulation of the Stokes problem*. SIAM J. Numer. Anal., **44**(2) (2007) 826–850.

[14] C. Bernardi, M. Dauge, and Y. Maday, *Spectral Methods for Axisymmetric Domains*. Gauthier-Villars, Éditions Scientifiques et Médicales Elsevier, Paris 1999.

[15] F. Brezzi, and M. Fortin, *Mixed and Hybrid Finite Element Methods*. Springer Verlag, New York 1991.

[16] R. Bürger, R. Ruiz-Baier, and H. Torres, *A stabilized finite volume element formulation for sedimentation–consolidation processes*, SIAM J. Sci. Comput., **34** (2012) B265–B289.

[17] J.H. Carneiro de Araujo, and V. Ruas, *A stable finite element method for the axisymmetric three-field Stokes system*. Comput. Methods Appl. Mech. Engrg. **164** (1998) 267–286.

[18] P. Clément, *Approximation by finite element functions using local regularisation*. RAIRO Modél. Math. Anal. Numér., **9** (1975) 77–84.

[19] V.J. Ervin, *Approximation of axisymmetric Darcy flow using mixed finite element methods*, SIAM J. Numer. Anal., **51**(3) (2013) 1421–1442.

[20] V.J. Ervin, *Approximation of coupled Stokes-Darcy flow in an axisymmetric domain*, Comput. Methods Appl. Mech. Engrg., **258**(1) (2013) 96–108.

[21] G.N. Gatica, *A Simple Introduction to the Mixed Finite Element Method. Theory and Applications*. Springer Briefs in Mathematics, Springer, Cham Heidelberg New York Dordrecht London, 2014.

[22] G.N. Gatica, A. Márquez, R. Oyarzúa, and R. Rebolledo, *Analysis of an augmented fully-mixed approach for the coupling of quasi-Newtonian fluids and porous media*. Comput. Methods Appl. Mech. Engrg., 270(1) (2014) 76–112.

[23] G.N. Gatica, L.F. Gatica, and A. Márquez, *Analysis of a pseudostress-based mixed finite element method for the Brinkman model of porous media flow*. Numer. Math., 126(4) (2014) 635–677.

[24] J. Gopalakrishnan, and J. Pasciak, *The convergence of V-cycle multigrid algorithms for axisymmetric Laplace and Maxwell equations*. Math. Comp., **75** (2006) 1697–1719.

[25] R. Grauer, and T.C. Sideris, *Numerical computation of 3D incompressible ideal fluids with swirl*. Phys. Rev. Lett., **67** (1991) 3511–3514.

[26] A. Guardone, and L. Vigevano, *Finite element/volume solution to axisymmetric conservation laws*. J. Comput. Phys., **224** (2007) 489–518.

[27] A. Kufner, *Weighted Sobolev Spaces*. Wiley, New York 1983.

[28] P. Lacoste, *Solution of Maxwell equation in axisymmetric geometry by Fourier series decomposition and by use of $H(rot)$ conforming finite element*. Numer. Math., **84** (2000) 577–609.

[29] Y.-J. Lee, and H. Li, *Axisymmetric Stokes equations in polygonal domains: Regularity and finite element approximations*. Comput. Math. Appl., **64** (2012) 3500–3521.

[30] Y.-J. Lee, and H. Li, *On stability, accuracy, and fast solvers for finite element approximations of the ax-*

isymmetric Stokes problem by Hood-Taylor elements. SIAM J. Numer. Anal., **49**(2) (2011) 668–691.

[31] J.-G. Liu, and W.-C. Wang, *Convergence analysis of the energy and helicity preserving scheme for axisymmetric flows*. SIAM J. Numer. Anal., **44**(6) (2006) 2456–2480.

[32] B. Mercier, and G. Raugel, *Resolution d'un problème aux limites dans un ouvert axisymétrique par éléments finis en r, z et séries de Fourier en θ*. RAIRO Anal. Numér., **16** (1982) 405–461.

[33] G. Pontrelli, *Blood flow through an axisymmetric stenosis*, Proc. Intn. Mech. Engrs., **215** (2001) H01–H10.

[34] V. Ruas, *Mixed finite element methods with discontinuous pressures for the axisymmetric Stokes problem*. ZAMM Z. Angew. Math. Mech., **83** (2003) 249–264.

[35] P.N. Tandon, and U.V.S. Rana, *A new model for blood flow through an artery with axisymmetric stenosis*, Int. J. Biomed. Comput., **38** (1995) 257–267.

[36] P. Vassilevski, and U. Villa, *A mixed formulation for the Brinkman problem*. SIAM J. Numer. Anal., **52**(1) (2014) 258–281.